


Article

Development of PA6/GF Long-Fiber-Reinforced Thermoplastic Composites Using Pultrusion and Direct Extrusion Manufacturing Processes

Sung-Eun Kim ^{1,2}, Jun-Geol Ahn ^{1,2}, Seungjae Ahn ³, Do-Hyung Park ⁴, Da-Hee Choi ⁴, Jae-Chul Lee ², Hyun-Ik Yang ^{1,*}  and Ki-Young Kim ^{2,*}

¹ Department of Mechanical Design Engineering, Hanyang University, Seoul 04763, Korea; kaste@hanyang.ac.kr (S.-E.K.); anjonkoul@kitech.re.kr (J.-G.A.)

² Material & Component Convergence R&D Department, Korea Institute of Industrial Technology (KITECH), Ansan-si 15588, Korea; jc2@kitech.re.kr

³ ESC Coprosperity Division, Korea High Tech Textile Research Institute (KOTERI), Yangju-si 11410, Korea; sjahn@koteri.re.kr

⁴ Development Team, Toray Advanced Materials Korea, Gumi-si 39422, Korea; ehgud0827@torayamk.com (D.-H.P.); choidahee@torayamk.com (D.-H.C.)

* Correspondence: skynet@hanyang.ac.kr (H.-I.Y.); kkim@kitech.re.kr (K.-Y.K.)

Abstract: The mechanical properties of polyamide 6 glass fiber (PA6/GF) long-fiber-reinforced thermoplastic (LFT) composites were characterized by studying the process conditions in terms of manufacturing methods (direct extrusion and pultrusion) and material characteristics (void content and fiber volume fraction). The LFT composites prepared through the pultrusion process have higher mechanical properties than those prepared via the direct extrusion process. The PA6/GF composite prepared via pultrusion had the tensile and flexural strengths of 233 MPa and 338 MPa, respectively. The impact strength measured using the Izod method was 296 J/m, which is 64% higher than that of the composite fabricated via the direct process. The optical microscope images showed that the glass fiber length of the pultruded composites is longer than the fiber length of the direct composites, leading to higher mechanical properties of the LFT composites prepared through the pultrusion process. Moreover, the interfacial shear strength between the resin and the fiber, measured via single fiber pullout tests, can account for the higher fiber reinforcing efficiency. If the void content of a composite is sufficiently small to not be detrimental to the composites, the mechanical properties are observed to be proportional to the fiber volume fraction of the composites.

Keywords: glass fiber; polyamide 6; fiber-reinforced composite; thermoplastics; mechanical properties



Citation: Kim, S.-E.; Ahn, J.-G.; Ahn, S.; Park, D.-H.; Choi, D.-H.; Lee, J.-C.; Yang, H.-I.; Kim, K.-Y. Development of PA6/GF Long-Fiber-Reinforced Thermoplastic Composites Using Pultrusion and Direct Extrusion Manufacturing Processes. *Appl. Sci.* **2022**, *12*, 4838. <https://doi.org/10.3390/app12104838>

Academic Editor: Han-Yong Jeon

Received: 1 April 2022

Accepted: 4 May 2022

Published: 10 May 2022

Publisher's Note: MDPI stays neutral with regard to jurisdictional claims in published maps and institutional affiliations.



Copyright: © 2022 by the authors. Licensee MDPI, Basel, Switzerland. This article is an open access article distributed under the terms and conditions of the Creative Commons Attribution (CC BY) license (<https://creativecommons.org/licenses/by/4.0/>).

1. Introduction

Recently, fiber-reinforced composite materials have attracted considerable attention in various industrial fields, such as automobiles, aerospace, vessels, sports, military, and electronics, owing to their characteristics, such as good mechanical properties, damping, low density, and formability [1–3]. Fiber-reinforced composites consist of reinforcing fibers, such as carbon fibers, glass fibers, or aramid fibers, and a polymer matrix made of thermoset or thermoplastic materials. The reinforcing fibers have intrinsic physical properties that provide high strength, modulus, and low density, whereas the polymer matrix transfers the internal force between one fiber and another in composite materials.

Thermoplastic materials are particularly advantageous in terms of impact resistance, reusability, and high productivity owing to their physical and chemical structures. Among thermoplastic materials, polyamide 6 (PA6) has often been used as the matrix of composites because it can provide not only a low cost but also advantageous mechanical properties at relatively high temperatures. Composites composed of PA6 and glass fibers have been used in research and industrial fields [4–7]. However, the intrinsic tensile and flexural

properties of thermoplastic materials are inferior to those of thermoset materials. The relationship between the fiber length and mechanical properties has been studied for decades to solve these problems [8]. Long-fiber-reinforced thermoplastic (LFT) composites are widely utilized because they have better mechanical properties than short fibers, which are utilized in short-fiber-reinforced thermoplastics [9,10]. Furthermore, LFT can have significantly high fiber content [4]. Increasing the fiber content is expected to improve the mechanical properties of discontinuous fiber composites.

In this study, the manufacturing methods of LFT composites were classified into pultrusion and direct processes to study their effects on the fiber length of PA6/GF composites. The pultrusion process typically leads to improved mechanical properties because it induces a longer fiber length than the direct process for reinforcing the fibers. On the other hand, the direct process is less affected by the melt viscosity than the pultrusion method. Therefore, there are many types of resins that can be manufactured using the direct process, including high melting point viscous polymers such as Polyether ether ketone (PEEK), Polyphenylene Sulfide (PPS), Polyesterimide (PEI), etc. These polymers can be economically produced through the direct process. However, composites prepared via the direct process show notably poor mechanical properties, such as flexural strength, tensile strength, and impact strength. This study aimed to characterize the mechanical properties of PA6/GF composites in terms of the fiber content, resin type, and process.

2. Experiment

2.1. Materials

The PA6 resin products used were 1011 BRT and LUMID GP 1100A (W), which have low relative viscosities. They were obtained from Hyosung and LG Chem, respectively. To remove moisture, the PA6 resin was subjected to a drying process in a convection oven at 100 °C for 2 h. The reinforcing fiber used was EDR240-T835 glass fiber from Taishan Fiberglass Inc. (CTG). This fiber has good compatibility with the PA6 resin. The fiber diameter and linear density were 17 µm and 2400 tex, respectively.

Two types of GF/PA6 (1011 BRT, GP 1100A (W)) masterbatches were preferentially prepared with a fiber content of more than 50 wt% via two different processes. Table 1 lists the resin and fiber contents of the masterbatches. In Table 1 and other tables and figures, “P” indicates the pultrusion process, and “D” indicates the direct extrusion process. In addition, “B” indicates 1011 BRT, and “G” indicates GP 1100A (W). The PA6/GF composite specimens used for the mechanical tests were prepared via injection molding. In this process, the weight content of the glass fibers was controlled by adding pure PA6 resin to the masterbatches. The fiber content of each specimen used in this study for the mechanical tests was in the range of 40 wt% to 50 wt%.

Table 1. Fiber and resin weight contents of the GF/PA6 masterbatches.

Masterbatch (Process-Resin)	Fiber Content (wt%)	Resin Content (wt%)
P-B	56.2	43.8
P-G	61.4	38.6
D-B	58.8	41.2
D-G	65.1	34.9

2.2. Preparation of PA6/GF Composites

Figure 1 shows the pultrusion and direct processes performed in this study. In the pultrusion process, glass fibers are loaded from an extruder into an impregnation die containing melted resins, and the fibers are impregnated with resins while they pass through the impregnation die. Then, a tension roller pulls the impregnated fibers into a water cooling bath and pelletizer (Figure 1a). By contrast, the direct process uses two twin-screw extruder systems. First, PA6 pellets are supplied to the first extruder to melt the PA6 resin. This extruder then supplies the melted resin to the second extruder.

The second extruder compounds the PA6 resins and glass fibers. The masterbatch in this process was prepared by directly chopping the fibers inside the barrel and compounding them with the resins in the second extruder (Figure 1b). The difference in the fiber length of the composite is due to the fiber length of the masterbatch. In the case of pultrusion, since the resin is melted with an extruder and the molten resin is impregnated into the roving glass fiber yarn to form a strand, damage to the glass fiber hardly occurs before pelletizing. On the other hand, in the case of direct extrusion, as the roving glass fiber yarn and molten resin are simultaneously fed into the second extruder, the glass fiber is cut due to shear force, screw element, and fiber–fiber interaction due to the flow of resin in the extruder. In the direct extrusion, the length of the fiberglass is already short before being pelletized as it forms strands and exits through a nozzle. Therefore, even if the masterbatch manufactured by the two processes has the same length of 12 mm, the length of the embedded glass fiber is longer in the masterbatch manufactured by pultrusion. Tables 2 and 3 show the extruder temperature settings for the pultrusion and direct processes, respectively. The process temperature was set to consider the thermal and rheological properties of the PA6 resins. The masterbatches were used to measure the mechanical properties of the specimens using injection molding.

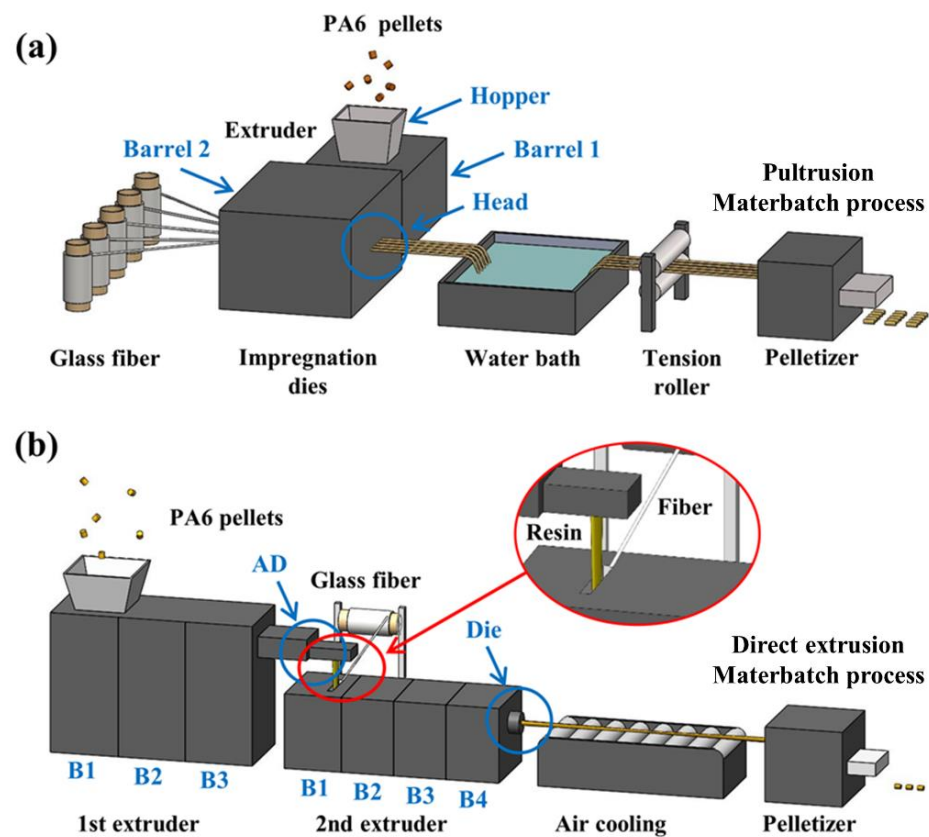


Figure 1. Masterbatch processing schematics of (a) the pultrusion process and (b) the direct extrusion process.

Table 2. Extruder temperature profile for the LFT pultrusion manufacturing processes.

Pultrusion	Hopper	Barrel 1	Barrel 2	Head
Temperature (°C)	250	260	270	270

Table 3. Extruder temperature profile for the LFT direct extrusion manufacturing processes.

Direct Extrusion	1 Extruder				2 Extruder				
	B1	B2	B3	AD	B1	B2	B3	B4	Die
Temperature (°C)	240	245	250	255	240	245	250	255	260

2.3. Test Methods

Differential scanning calorimetry (DSC) (TA Instruments, Q100) and thermogravimetric analysis (TGA) (TA Instruments, Q500) were performed to determine the thermal properties of the PA6 resins in a nitrogen atmosphere. DSC analysis was performed in a scan range from room temperature (RT) to 300 °C at a scan rate of 10 °C/min. TGA was performed in the scan range from RT to 800 °C at a scan rate of 20 °C/min.

A rotational rheometer (TA Instruments, DHR-1) was used to measure the viscoelasticity of the resin. The PA6 film was prepared using a hot-press process at 250 °C for 15 min. Rheometer tests were performed in the scan range of 230–290 °C at a scan rate of 2 °C/min. The maximum torque was 150 mN·m, and the strain was 5% at 1 Hz.

The interfacial shear strength (IFSS) between the PA6 resin and the glass fiber was measured using a single-fiber pullout test, which was performed using a self-made pullout test system (Figure 2). The self-made pullout test system comprised a micro-tensile tester (DAEYONG M.T.C., EMC-001) connected to an optical microscope (OM) (Olympus, CKX41). The maximum force (F_{max}) was determined from the force–displacement curve. This maximum force originates from the debonding and friction between the resin and the fiber [11–13]. The IFSS is calculated as follows:

$$IFSS = \frac{F_{max}}{\pi d_f L_e} \quad (1)$$

where d_f is the fiber diameter with a value of 17 µm. The range of embedded fiber length (L_e) was 200 to 300 µm. The crosshead speed of the micro-tensile tester was 0.5 mm/min at RT.

**Figure 2.** Single-fiber pullout test setting.

The physical properties of the PA6/GF composites, such as the fiber weight content, matrix weight content, void content, and fiber volume content, were measured via a burning process using a muffle furnace (DAIHAN, WiseTherm®) according to the ASTM D3171-06 standard. The residues of the PA6/GF composite were then diffused in distilled water to measure the fiber length of the composite. The residual solution was dried in a convection oven at 100 °C for 1 h. The residues were observed using the OM (Olympus, CKX41). Furthermore, the fiber length of the composites in the residues was analyzed using ImageJ®, an imaging analysis program.

The tensile strength was measured in accordance with the ASTM D638 standard using a universal testing machine (Tinius Olsen, H5KT). The flexural strength was measured

using ASTM D790, which is a three-point bending test. The impact strength was measured using ASTM D256, which is an Izod impact test.

After the tensile test, the fracture surfaces of the PA6/GF composites were inspected using field-emission scanning electron microscopy (FE-SEM) (Hitachi, SU8010). The surfaces of the fractured composites were coated with platinum via sputtering to prevent charging.

3. Results and Discussion

3.1. Characteristics of PA6 Resin

The thermal and viscoelastic properties of the two types of PA6 resins—1011 BRT and GP 1100A (W)—were used to optimize the manufacturing conditions. Figure 3 shows the thermal properties of the two types of PA6 resins obtained using DSC and TGA. The DSC results showed a melting temperature (T_m) of approximately 220 °C for each resin. Regardless of the resin type, the process temperature must be above 220 °C. The initial decomposition temperatures ($T_{5\%}$) of 1011 BRT and GP 1100A (W) were 393 °C and 404 °C, respectively, according to the TGA results. This information regarding thermal properties allows appropriate process temperatures to be set, preventing the degradation of mechanical properties that would be caused by thermal decomposition.

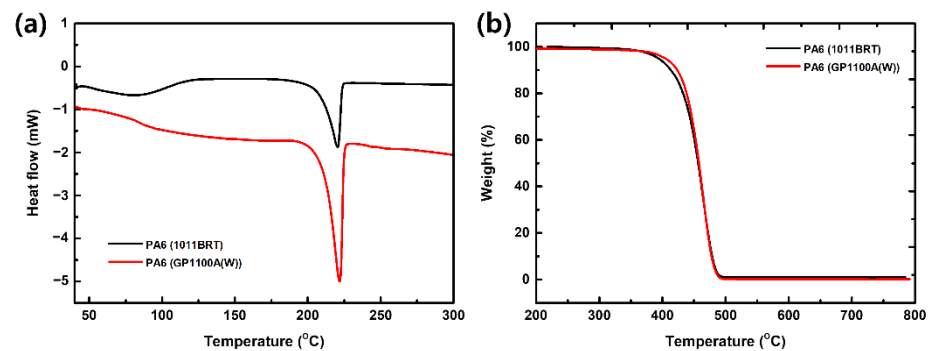


Figure 3. Analyses of PA6 resins: (a) DSC and (b) TGA.

The viscoelastic properties of the PA6 resins are shown in Figure 4. Rotational rheometry was performed at temperatures above the melting temperature of the PA film. Consequently, the storage modulus increased with increasing temperature. This phenomenon was particularly apparent at temperatures above 270 °C. However, the loss modulus decreases with increasing temperature. This increase in the storage modulus and decrease in the loss modulus indicate that the melting resin has a more solid-like property above 270 °C. These property changes may reduce the workability of pultrusion and direct processes by inducing difficult wetting and impregnation with resins. The process temperature was set below 270 °C in both the manufacturing processes to optimize the process conditions.

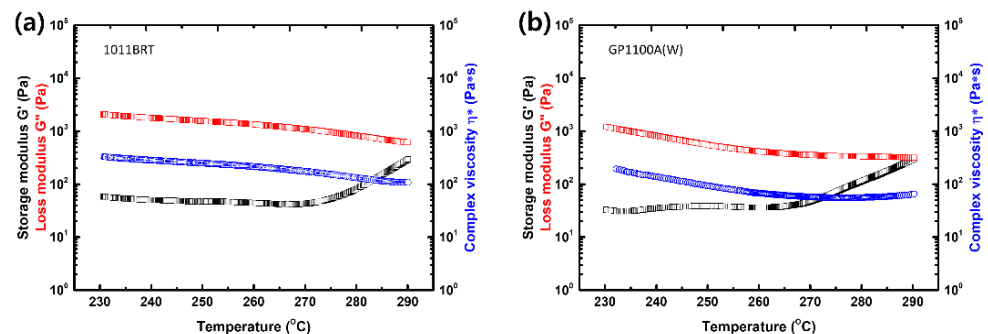


Figure 4. Results of rotational rheometer tests for PA6 resin: (a) 1011 BRT and (b) GP 1100A (W).

3.2. Interface between PA6 and Glass Fibers

The interfacial characteristics were measured using a single fiber pullout test, which indirectly predicted the mechanical properties of the composites. Figure 5a shows the scheme of the single fiber pullout test, in which a single glass fiber composite was constructed on a slide glass substrate. A force was applied to the glass fiber under unidirectional tension until the glass fiber was pulled out of the adhesive resin. This phenomenon was observed using an OM capable of capturing images in real time (Figure 5b). Figure 6 shows a graph of the embedded fiber length (L_e) versus maximum force (F_{max}). The embedded fiber length is nearly proportional to the maximum force within its range (100–200 μm). The IFSS between 1011 BRT and the glass fibers was higher than that between GP 1100A (W) and the glass fibers (Table 4). Thus, these results aid the selection of appropriate resins for the manufacturing processes, as they indicate that a lower IFSS could ease the initiation of microcracks when the composite is stressed, leading to a degradation in the mechanical properties of the composite.

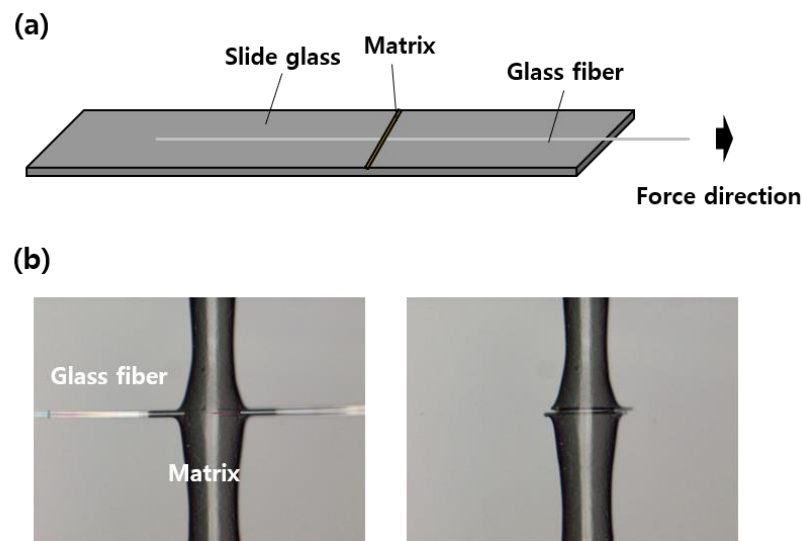


Figure 5. Single-fiber pullout test: (a) specimen composition and (b) OM images before and after the experiment.

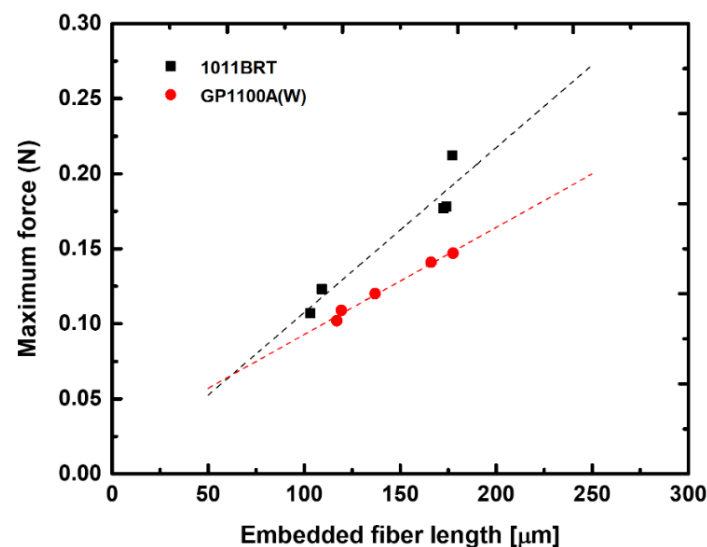


Figure 6. Results of the single fiber pullout test.

Table 4. IFSS calculation result and standard deviation of the GF and PA6 interface.

Sample	IFSS (MPa)	Standard Deviation
1011 BRT	20.27	1.45
GP 1100A (W)	16.25	0.59

3.3. Characteristics of Composites

After the pultrusion and direct processes, the PA6/GF composite specimens were injection-molded by adjusting the glass fiber weight content (target—40 wt%, 50 wt%) and resin types (1011 BRT, GP 1100A (W)). Table 5 shows the physical characteristics of eight types of composites (Processes—P and D, resin types—B and G, target fiber contents—40 wt% and 50 wt%). Although the target fiber contents could not be exactly matched in some conditions, the error did not significantly impair the overall process of determining the optimized conditions. The glass fiber and resin weight contents, density, fiber volume, and void content of the PA6/GF composites are summarized in Table 5 with regard to the processes, resin types, and target weight contents. The fiber volume content (V_f) of the composites increased with increasing fiber weight content. The density of the composites was closely related to the void content in the materials. For composites with similar void contents, the composite density increases with increasing fiber weight content (W_f). In addition, composites with a low void content generally have a higher density than those with a high void content. However, several composite voids are defects that significantly degrade the mechanical properties. Regarding the physical characteristics, all the samples were expected to have excellent mechanical properties because they had a relatively low void content.

Table 5. Physical characteristics of the GF/PA6 specimens.

Specimens (Process-Resin-Fiber Content)	Fiber Content (wt%)	Resin Content (wt%)	Density (g/cc)	Fiber Volume Content (vol%)	Void Content (%)
P-B-40	38.9	61.1	1.419	21.55	2.37
P-B-50	47.4	52.6	1.515	28.06	2.10
P-G-40	40.0	60.0	1.409	21.89	3.03
P-G-50	51.7	48.3	1.581	31.96	1.66
D-B-40	33.8	66.2	1.346	17.77	4.04
D-B-50	47.6	52.4	1.504	27.94	2.87
D-G-40	41.2	58.8	1.429	22.97	2.65
D-G-50	53.1	46.9	1.551	32.16	3.42

The mechanical properties of composites, such as their strengths and modulus, are generally proportional to their fiber volume content. Table 6 shows the mechanical properties of one reference composite and eight types of composites. This phenomenon can be observed in Figure 7, which shows the relationship between the mechanical properties of the composite, such as tensile and flexural characteristics, and the fiber volume content. These graphs indicate that composites fabricated via the pultrusion process have better mechanical properties than those fabricated via the direct process. This was more apparent for the impact strength than for the tensile and flexural strengths (Figure 8). The increment in the modulus is dramatically higher than that of the strength with increasing fiber volume content. Figure 9 also shows the increment rate of the mechanical properties when the target fiber volume fraction increases from 40 wt% to 50 wt%. These results indicate that the fiber volume fraction has a greater influence on the modulus of the composites than the mean fiber length does [14]. Furthermore, the fiber lengths obtained from the pultrusion and direct processes were measured and compared. Figure 10 shows the OM images of the glass fibers after the burning process. The fiber lengths of the composites were observed to be hundreds of micrometers in the OM images. Generally, the decrease in the fiber length

of the composites is influenced by the increase in the interactions among the fiber–fiber, fiber–polymer, and fiber–processing-equipment surface wall, which is more significant for high-volume content composites [13–15]. In these images, the mean fiber length of the composites prepared via the pultrusion process was longer than that of the composites prepared via the direct process. However, all the composites have an outstanding interface between the fiber and the matrix regardless of their manufacturing process (Figure 11). This is due to the compatibility of the glass fibers with the PA6 resins.

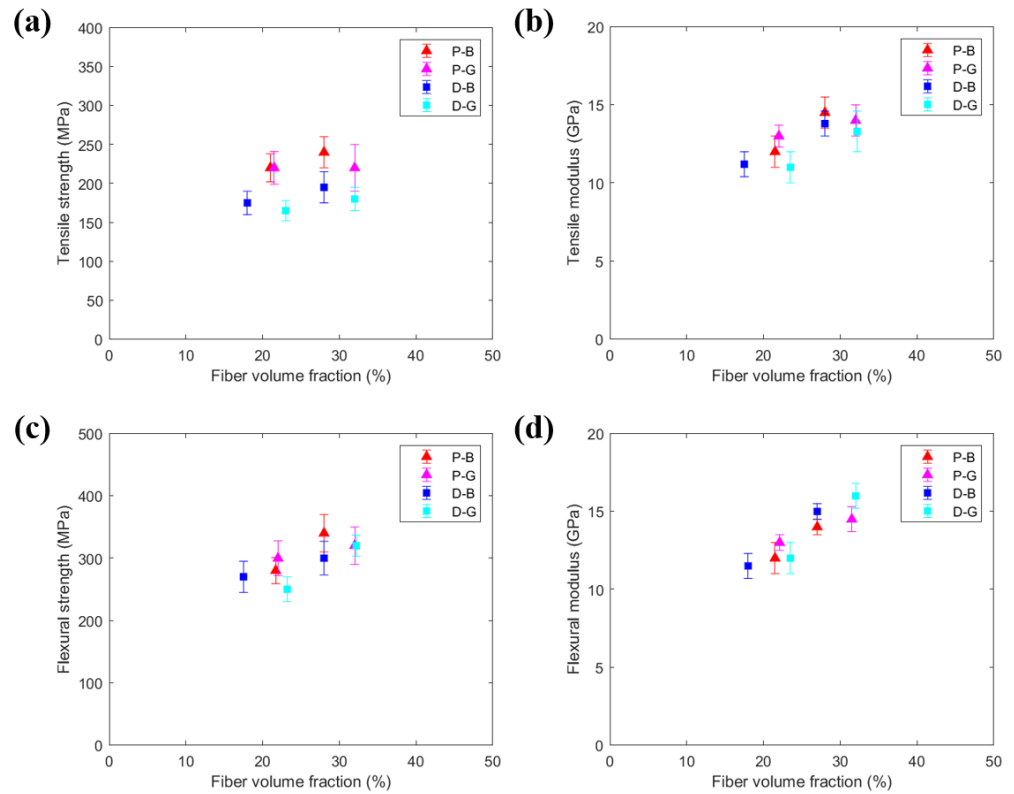


Figure 7. Scatter diagrams of the tensile and flexural properties of the GF/PA6 specimens by fiber volume fraction: (a) tensile strength; (b) tensile modulus; (c) flexural strength; (d) flexural modulus.

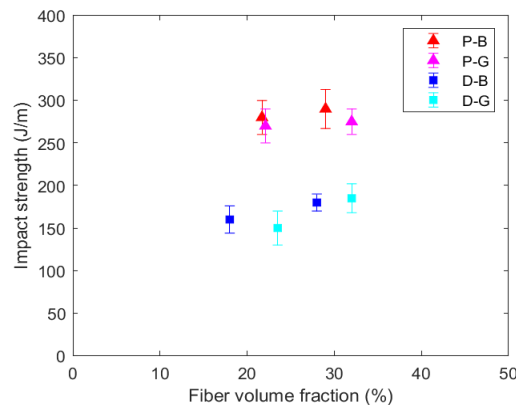


Figure 8. Scatter diagram of the impact strength of the GF/PA6 specimens by fiber volume fraction.

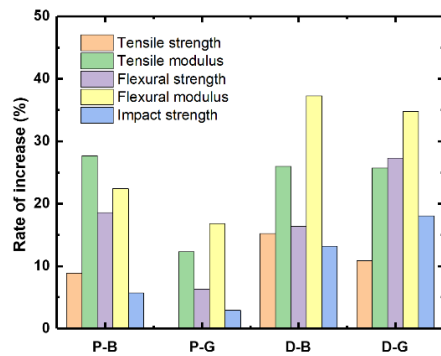


Figure 9. Increase rate of the mechanical properties of the GF/PA6 specimen (when increasing fiber content from 40 wt% to 50 wt%).

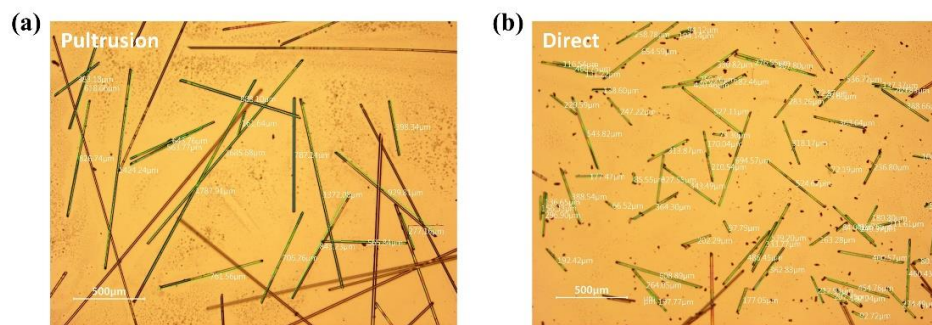


Figure 10. OM images of the GF fiber lengths from the pultrusion and direct extrusion processes: (a) pultrusion; (b) direct.

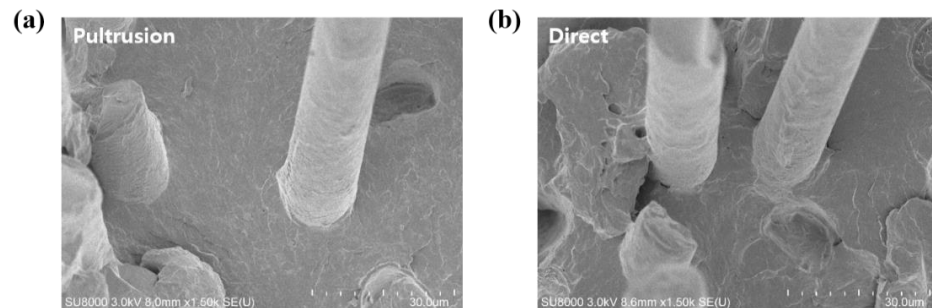


Figure 11. SEM images of the GF/PA6 interface from the pultrusion and direct extrusion processes: (a) pultrusion; (b) direct.

Table 6. Mechanical properties of the GF/PA6 specimens.

Specimens (Process-Resin-Fiber Content)	Tensile Strength (MPa)	Tensile Modulus (GPa)	Flexural Strength (MPa)	Flexural Modulus (GPa)	Impact Strength (J/m)
P-Ref-50 *	220	-	345	-	266
P-B-40	214	11.2	285	11.6	280
P-B-50	233	14.3	338	14.2	296
P-G-40	214	12.2	301	12.5	275
P-G-50	214	13.7	320	14.6	283
D-B-40	171	10.4	263	11.0	159
D-B-50	197	13.7	306	15.1	180
D-G-40	166	10.5	249	11.8	155
D-G-50	184	13.2	317	15.9	183

* Reference products, PA6/GF (fiber content 50 wt%), Verton1 PF-700-100, produced by LNP. Engineering Plastics, prepared by pultrusion [4].

3.4. Fiber Efficiency

The fiber efficiency coefficient is an index that can estimate the reinforcing effect of increasing the GF content. Fu et al. presented a modified rule of mixtures equation for the fiber efficiency factor in discontinuous short fiber-reinforced composites [14,15]. In addition, Ahn estimated the effect of LFT on the fiber content, length, and orientation using a modified rule of mixtures equation [16]. The modified rule of the mixture equation is as follows:

$$\lambda_{\sigma} = \frac{\sigma_c - \sigma_m(1 - V_f)}{\sigma_f V_f} \quad (2)$$

$$\lambda_E = \frac{E_c - E_m(1 - V_f)}{E_f V_f} \quad (3)$$

where λ_{σ} is the fiber efficiency factor for the tensile strength of the composite, σ_c , σ_m , and σ_f are the tensile strengths of the composites, matrices, and fibers, respectively, λ_E is the fiber efficiency factor of the tensile modulus of the composite, and E_c , E_m , and E_f are the tensile modulus of the composites, matrices, and fibers, respectively.

Tables 7 and 8 show the fiber efficiency results for the PA6/GF LFT composites. PA6/GF-P refers to the specimen prepared via the pultrusion process, and PA6/GF-D refers to the specimen prepared via the direct extrusion process. High λ_{σ} and λ_E values can lead to a significant increase in the mechanical properties of the composites. In most cases listed in Table 7; Table 8, the fiber efficiency factor decreased as the fiber content increased from 40 wt% to 50 wt%. This indicates that, as the fiber content is further increased, the increase in the mechanical properties can be less predictable, which is more pronounced in λ_{σ} than in λ_E . The pultrusion process shows a higher λ_{σ} than the direct extrusion process. Therefore, a higher tensile strength can be expected in the pultrusion process than in the direct extrusion process, and the pultrusion system is a more efficient manufacturing method for the GF/PA6 LFTs.

Table 7. Fiber efficiency factors of 1011 BRT.

	P-B-40	P-B-50	D-B-40	D-B-50
λ_{σ}	0.2155	0.1933	0.1956	0.1572
λ_E	0.6176	0.6401	0.6774	0.6121

Table 8. Fiber efficiency factors of GP 1100A (W).

	P-G-40	P-G-50	D-G-40	D-G-50
λ_{σ}	0.2181	0.1548	0.1490	0.1273
λ_E	0.6738	0.5394	0.5380	0.5140

4. Conclusions

This study aimed to optimize the mechanical properties of PA6/GF composites in terms of process conditions, such as process type, resin type, and fiber weight content. Based on the thermal and rheological properties of PA6 resins, PA6/GF composites were fabricated at temperatures below 270 °C. Compared to the pultrusion process, the direct extrusion process has a shorter fiber length because the fibers and resin are cut while entangled with the screw. Therefore, composites prepared via the pultrusion process have better mechanical properties than those prepared via the direct process because of their longer mean fiber length. The optimal combination of resins and fibers to prepare composites is directly related to the mechanical properties of the composite through its interface features. The results of the single-fiber pullout test demonstrated that the 1011 BRT resin is better than the GP 1100A (W) resin in our system. The composites prepared using the 1011 BRT resin were observed to have excellent mechanical properties. The fiber efficiency results of both process methods are higher in the pultrusion process than

in the direct extrusion process. These results indicate that the pultrusion process is a more efficient process in terms of mechanical properties. This study provides guidance on the types and processes of resins that can be altered to achieve the desired mechanical properties of PA6/GF.

Author Contributions: Conceptualization, S.-E.K., D.-H.P., and D.-H.C.; methodology, S.-E.K. and J.-G.A.; validation, J.-G.A., S.A., J.-C.L., and K.-Y.K.; formal analysis, S.-E.K.; investigation, D.-H.P. and D.-H.C.; resources, H.-I.Y. and K.-Y.K.; data curation, S.-E.K. and K.-Y.K.; writing—original draft preparation, S.-E.K. and J.-G.A.; writing—review and editing, H.-I.Y. and K.-Y.K.; visualization, S.-E.K.; supervision, H.-I.Y.; project administration, K.-Y.K.; funding acquisition, K.-Y.K. All authors have read and agreed to the published version of the manuscript.

Funding: This research was supported by the Technology Innovation Program (Parts and Materials Technology Development) (20011408, Development of thermoplastic composite material and part molding process technology for lightweight hydrogen electric vehicle electrical parts) funded by the Ministry of Trade, Industry, and Energy (MOTIE, Republic of Korea).

Institutional Review Board Statement: Not applicable.

Informed Consent Statement: Not applicable.

Data Availability Statement: Data sharing is not applicable.

Conflicts of Interest: The authors declare no conflict of interest.

References

1. Labatut, V.; Mayers, J.; Greene, T. Discontinuous LFT composites for structural aerospace applications. *JET Compos. Mag.* **2015**, *96*, 38–40.
2. Markarian, J. Long fibre reinforced thermoplastics continue growth in automotive. *Plast. Addit. Compd.* **2007**, *9*, 20–24. [[CrossRef](#)]
3. Thattai parthasarathy, K.B.; Pillay, S.; Ning, H.; Vaidya, U. Process simulation, design and manufacturing of a long fiber thermoplastic composite for mass transit application. *Compos. Part A Appl. Sci. Manuf.* **2008**, *39*, 1512–1521. [[CrossRef](#)]
4. Han, K.Q.; Liu, Z.J.; Yu, M.H. Preparation and mechanical properties of long glass fiber reinforced PA6 composites prepared by a novel process. *Macromol. Mater. Eng.* **2005**, *290*, 688–694. [[CrossRef](#)]
5. Akkapeddi, M.K. Glass fiber reinforced polyamide-6 nanocomposites. *Polym. Compos.* **2000**, *21*, 576–585. [[CrossRef](#)]
6. Zuo, X.; Shao, H.; Zhang, D.; Hao, Z.; Guo, J. Effects of thermal-oxidative aging on the flammability and thermal-oxidative degradation kinetics of tris (tribromophenyl) cyanurate flame retardant PA6/LGF composites. *Polym. Degrad. Stab.* **2013**, *98*, 2774–2783. [[CrossRef](#)]
7. Zuo, X.; Zhang, K.; Lei, Y.; Qin, S.; Hao, Z.; Guo, J. Influence of thermooxidative aging on the static and dynamic mechanical properties of long-glass-fiber-reinforced polyamide 6 composites. *J. Appl. Polym. Sci.* **2013**, *131*. [[CrossRef](#)]
8. Thomason, J. The influence of fibre length, diameter and concentration on the impact performance of long glass-fibre reinforced polyamide 6,6. *Compos. Part A Appl. Sci. Manuf.* **2009**, *40*, 114–124. [[CrossRef](#)]
9. An, H.J.; Kim, J.S.; Kim, K.-Y.; Lim, D.Y.; Kim, D.H. Mechanical and thermal properties of long carbon fiber-reinforced polyamide 6 composites. *Fibers Polym.* **2014**, *15*, 2355–2359. [[CrossRef](#)]
10. Lee, E.S.; Kim, J.S.; Kim, K.Y.; Lim, D.Y.; Kim, D.H. Preparation of polypropylene composites reinforced with long carbon fibers and their properties. *Fibers Polym.* **2014**, *15*, 2613–2617. [[CrossRef](#)]
11. Marotzke, C. Influence of the fiber length on the stress transfer from glass and carbon fibers into a thermoplastic matrix in the pull-out test. *Compos. Interfaces* **1993**, *1*, 153–166. [[CrossRef](#)]
12. Singletary, J.; Baines, R.W.; Beckett, W.; Friedrich, K. Examination of fundamental assumptions of analytical modeling of fiber pullout test. *Mech. Adv. Mater. Struct.* **1997**, *4*, 95–112. [[CrossRef](#)]
13. Karsli, N.G.; Aytac, A. Tensile and thermomechanical properties of short carbon fiber reinforced polyamide 6 composites. *Compos. Part B Eng.* **2013**, *51*, 270–275. [[CrossRef](#)]
14. Fu, S.-Y.; Lauke, B.; Mäder, E.; Yue, C.-Y.; Hu, X. Tensile properties of short-glass-fiber- and short-carbon-fiber-reinforced polypropylene composites. *Compos. Part A Appl. Sci. Manuf.* **2000**, *31*, 1117–1125. [[CrossRef](#)]
15. Fu, S.-Y.; Hu, X.; Yue, C.-Y. Effects of fiber length and orientation distributions on the mechanical properties of short-fiber-reinforced polymers a review. *J. Soc. Mater. Sci. Japan* **1999**, *48*, 74–83. [[CrossRef](#)]
16. Ahn, S.; Lee, J.-C.; Kim, K.-Y. Preparation and Characterization of Glass-Fiber-Reinforced Modified Polyphenylene Oxide by a Direct Fiber Feeding Extrusion Process. *Appl. Sci.* **2021**, *11*, 10266. [[CrossRef](#)]